GEOGRAFICKÝ ČASOPIS / GEOGRAPHICAL JOURNAL 78 (2026) 4, 193-205
DOI: https://doi.org/10.31577/geogrcas.2026.78.4.01

INSTITUTE OF GEOGRAPHY SLOVAK ACADEMY OF SCIENCES

Geografický časopis
Geographical Journal

Assessing spatio-temporal changes in landscape structure: An index-based approach in a forested watershed

Mohsen Zabihi[1,*], Mehdi Shojaei[2], Alireza Motevalli[3], Raoof Mostafazadeh[4,*], Fatemeh Hashemi[3]

[1] Department of Watershed Management Engineering, Faculty of Natural Resources, Tarbiat Modares University, Tehran, Iran, mohsen_zabihi69@yahoo.com
[2] Department of Survey Engineering-Geographic Information Systems, Faculty of Civil Engineering, Lamei Gorgani Institute of Higher Education, Gorgan, Iran, mehdi.shojaee@yahoo.com
[3] Department of Agroecology, Aarhus University, Tjele, Denmark, arm@agro.au.dk, fh@agro.au.dk
[4] Department of Natural Resources, Member of Water Management Research Center, Faculty of Agriculture and Natural Resources, University of Mohaghegh Ardabili, Ardabil, Iran, raoofmostafazadeh@uma.ac.ir
* Corresponding author

Abstract

Land use composition and structure changes in an ecosystem originates from driving forces of landscape changes. Quantifying the landscape using different metrics helps to better understanding of processes and determining the driving forces of ecosystem changes. This study investigates land use changes in the Ramian watershed in Golestan province of Iran using a landscape metrics approach to assess spatial pattern shifts over 30 years. Landsat images from 1991, 2006, and 2021 were classified using the Support Vector Machine (SVM) algorithm, and land use maps were evaluated for accuracy using the Kappa coefficient and Overall Accuracy. Seventeen landscape metrics were analyzed at both landscape and class levels using FRAGSTATS and the eight-cell neighbourhood method. Forest cover declined from 61.06% (1991) to 58.31% (2021) but remained the dominant land use, while rainfed agriculture (8.16% to 20.24%) and residential areas (0.63% to 1.3%) increased, indicating land use expansion. Over 30 years, the landscape structure became more complex. While the total number of patches (NP) slightly decreased, the reduction in the Largest Patch Index (LPI) indicated the fragmentation of the dominant forest cover. Concurrently, the Interspersion and Juxtaposition Index (IJI) increased, indicating greater intermixing of land-use types. Results revealed a clear decline in natural land covers and an expansion of human-modified uses, leading to a more complex, dispersed, and subdivided landscape structure. These findings highlight the impact of human activities on landscape degradation, emphasizing fragmentation and the growing complexity of anthropogenic patches, which signal the need for targeted ecological restoration and sustainable management practices.

Key words:
landscape dynamics, land use change, ecological degradation, spatio-temporal analysis, forest management

1 INTRODUCTION

Landscape ecology, as a foundational discipline, investigates the relationships between spatial patterns and ecological processes across various scales (Turner, 1989). The development of quantitative metrics to characterize landscape structure has been a cornerstone of the field, enabling systematic analysis of fragmentation, connectivity, and heterogeneity (O'Neill et al., 1988; Pickett & Cadenasso, 1995; Gustafson, 1998). These theoretical frameworks established the importance of patch dynamics, edge effects, and the matrix in shaping ecological functions. Building upon this theoretical foundation, operational tools like Fragstats (McGarigal & Marks, 1995) were developed to compute a comprehensive suite of landscape metrics, translating abstract patterns into quantifiable indices. These tools became instrumental for characterizing landscape composition (e.g., percentage of landscape – PLAND) and configuration (e.g., patch density, edge density). Following these seminal works, subsequent research has widely adopted and refined the use of such metrics to diagnose land use/cover change (LUCC) impacts, assess habitat quality, and inform conservation planning (Wei et al., 2016; Sakieh & Salmanmahiny, 2016; Nie et al., 2023). This study builds upon this established lineage by employing a Fragstats-based, multi-metric approach to quantify spatio-temporal structural changes in a forested watershed, linking observed patterns to potential ecological consequences of anthropogenic pressure.

Landscape ecology helps understand how spatial patterns, like land use and connectivity, affect biodiversity, ecological functions, and nutrient flows (Mirzaei et al., 2018; Darvishi et al., 2024; McLeod et al., 2025). Remote sensing and spatial analysis allow researchers to evaluate land use composition and configuration, providing valuable indications into the distribution and connectivity of urban, agricultural, and natural areas (Baude et al., 2019; Diuk-Wasser et al., 2021; Alaei et al., 2024; Zabihi et al., 2025). Spatio-temporal analysis of landscape changes is essential for

evaluating the ecological impacts of land use changes and informing sustainable land management strategies (Alaei et al., 2022). A landscape, in the context of landscape ecology, refers to the spatial arrangement of land use types and natural elements within a given area (Huggett & Cheseman, 2002; Herold et al., 2005). It comprises three key aspects: structure, function, and change over time (Forman, 2008). Structure refers to the organization of landscape elements, including patches, corridors, and the matrix. Patches are distinct, homogeneous areas, while corridors aid species movement and nutrient flow (Mony et al., 2024; Heydari-Guran & Ghasidian, 2024). The matrix, as the dominant land cover, affects ecological function, and ecotones, or transitional zones, are crucial for species exchange and energy transfer (Ortiz-Colin & Hulshof, 2024). Function involves the interactions among these elements, such as energy flow, nutrient cycling, and species dynamics (Zhang et al., 2023). Landscape change, driven by both natural processes and human activities, highlights the dynamic nature of ecosystems (Forman, 2008; Azareh et al., 2024). Landscape metrics are essential tools for quantifying structural characteristics such as fragmentation, connectivity, and patch distribution, providing critical insights into the ecological effects of land use changes (Lambin et al., 2003; Uddin et al., 2018). Key metrics, including patch density, edge density, and the largest patch index, are widely used to assess habitat loss and connectivity (Walz, 2011). Longitudinal studies using these metrics help track fragmentation trends and changes in habitat connectivity, aiding land use planning and conservation efforts (Blyth et al., 2011; Van Vliet et al., 2011). Integrating landscape metrics into modeling helps researchers predict future land use patterns, identify vulnerable areas, and assess the impacts of climatic and anthropogenic factors (da Silva et al., 2021; Chang et al., 2021). Land use changes, such as urbanization, agricultural expansion, and deforestation, profoundly impact landscape structure and ecological processes. These transformations often lead to fragmentation, habitat loss, and biodiversity decline (Chiesa et al., 2009; Mirzaei et al., 2018). Urbanization, for instance, increases edge density and reduces patch size, resulting in more isolated habitats that hinder species movement and population sustainability (Lambin et al., 2003; Uddin et al., 2018).

Numerous studies have used landscape metrics to quantify urban and agricultural impacts. Bihamta Toosi et al. (2014) found urban expansion in Isfahan fragmented agricultural lands, reducing patch sizes. Dezhkam and Jabbarian Amiri (2015) reported that urban growth in Rasht increased landscape heterogeneity and patch irregularity. Rafiee et al. (2009) observed a significant loss of green spaces in Mashhad due to urbanization. Studies in Brazil (De Barros Ferraz et al., 2005) and China (Deng et al., 2009) show how urban sprawl and deforestation increased fragmentation and reduced habitat connectivity. In agricultural landscapes, Kumar et al. (2018) found forest conversion to agriculture in India increased fragmentation, while Zabihi et al. (2020) noted similar effects in Iran due to agricultural and residential expansion. Cervelli et al. (2025) analyzed land use changes in Italy's Sorrento Peninsula, where farmland declined 20% and buildings doubled. Yang et al. (2025) studied land use shifts in a Chinese river basin, finding urban areas grew as cropland shrank. Khan and Chen (2025) analyzed land changes in Khyber Pakhtunkhwa, noting a 138% urban growth linked to higher temperatures and ecosystem decline. Vlachogianni et al. (2025) studied land use changes in the Ptolemais lignite mines, Greece. Satellite data from 1988 to 2023 showed mining altered both the site and surroundings, highlighting environmental impacts and reclamation challenges. Human activities are driving fragmentation, habitat loss, and the decline of green spaces, threatening biodiversity and ecosystem stability, which underscores the need for effective land use planning. However, there are gaps in research regarding the impact of environmental pressures on landscape structure in mountainous forests. While many studies measure fragmentation, they often lack insight into its functional effects. Investigating land use transitions and their cumulative impact on ecosystems is essential for informing sustainable land management policies and ensuring long-term landscape stability.

Long-term assessment of landscape structure and land uses are crucial for understanding the cumulative effects of land use transformations and identifying most influencing driving forces of change. By analyzing landscape metrics over extended periods, researchers can monitor trends in fragmentation, habitat loss, and biodiversity shifts. This longitudinal analysis allows for the detection of gradual changes that may not be immediately apparent, helping to identify early signs of ecological degradation. Furthermore, tracking these trends enables researchers to assess the effectiveness of conservation strategies, predict future landscape dynamics, and develop more targeted interventions. By understanding how fragmentation and habitat loss evolve over time, researchers can provide crucial data for policymakers and land managers to make informed decisions that support biodiversity conservation and ecosystem resilience. Similarly, Zabihi et al. (2019) found that non-forest land uses expanded in the Talar watershed, worsening fragmentation.

Despite the recognized global importance of forested watersheds for biodiversity and ecosystem services, these areas face intensifying anthropogenic pressures. In the Hyrcanian forests of northern Iran (a biodiversity hotspot) agricultural expansion and urbanization are driving rapid land use/cover change (LUCC). This transformation, particularly evident in watersheds like Ramian in Golestan province, remains insufficiently quantified in terms of its precise impact on landscape structural integrity. The consequent habitat fragmentation, increased edge effects, and loss of connectivity threaten ecological resilience and watershed functions (e.g., flood mitigation, soil conservation), yet a detailed, metric-based assessment of these spatio-temporal structural changes is lacking for this critical region.

While previous studies have documented LUCC in the region (e.g., Zabihi et al., 2020), a significant gap exists in applying a comprehensive suite of landscape metrics to simultaneously assess composition, configuration, and connectivity over multiple time periods. Most studies either focus on single metrics, lack a long-term temporal analysis (e.g., 30-year span), or do not integrate class-level and landscape-level diagnostics to disentangle the differential impacts on various land use types. Furthermore, there is limited insight into how these structural changes specifically manifest in mountainous, forest-dominated watersheds under mixed pressures of agriculture and settlement expansion, as opposed to predominantly urban-driven changes.

Addressing this gap is critical for several reasons. Scientifically, it provides a benchmark for understanding landscape evolution dynamics in semi-humid forest ecosystems under pressure. Methodologically, it demonstrates the utility of an

integrated, multi-metric approach for robust landscape diagnosis. From an applied management perspective, quantifying fragmentation patterns and connectivity loss is essential for evidence-based conservation planning. The findings will directly inform local land-use policymakers and environmental managers in the Hyrcanian region, helping to prioritize areas for restoration, design ecological corridors, and develop strategies to mitigate soil erosion and hydrological disruption caused by landscape degradation.

Therefore, the primary objective of this study is to quantitatively assess the spatio-temporal changes in landscape structure within the Ramian watershed over a 30-year period (1991–2021). This main objective is achieved through the following specific aims: a) to map and quantify land use/cover changes for 1991, 2006, and 2021 using satellite imagery and the SVM algorithm; b) to analyze changes in landscape composition using metrics such as PLAND, CA, and LPI at both class and landscape levels; c) to evaluate changes in landscape configuration and connectivity using metrics including NP, PD, ED, LSI, IJI, and COHESION; d) to interpret the ecological implications of the observed structural changes and provide recommendations for sustainable watershed management.

2 MATERIAL AND METHODS

Study Area

The Ramian watershed, covering approximately 245 km^2, is located in the southern part of Ramian county in Golestan province. The climate is mountainous and semi-humid with an average annual precipitation of 680 mm and a daily temperature of 16.5 °C. Based on the De Martonne classification, the climate is considered humid (Sadoddin et al., 2010). According to the widely adopted Köppen–Geiger climate classification system, the area falls within the Csa category, characterized by a temperate climate with dry, hot summers and mild, wet winters, typical of the Mediterranean climate zone (Climate-Data.org. 2025). The Ghare-Chai River, which flows for 39 km, is the primary watercourse in the watershed. The area's average elevation is about 1305 m, and its average slope is approximately 40%. Forests dominate the land use, and the city of Ramian is the only urban area within the watershed. Figure 1 illustrates the geographical location of the watershed. The Ramian watershed is ecologically significant due to its diverse natural features and strategic location in Golestan province. Its mountainous terrain, with a mix of steep slopes and varying elevations, supports rich biodiversity, particularly in its forests, which play a crucial role in maintaining ecosystem services like water regulation and soil conservation. The watershed's semi-humid climate fosters a unique combination of flora and fauna, making it an essential region for environmental studies and conservation efforts. Additionally, the Ghare-Chai River provides vital water resources for the area, influencing both ecological dynamics and human livelihoods.

Methodology

Land use mapping

Toward the objective of this study, Landsat satellite images were obtained from the United States Geological Survey (USGS) website. For 1991 and 2006, Landsat 5 Thematic Mapper (TM) images were used, while for 2021, Landsat 8 Operational Land Imager (OLI)/Thermal Infrared Sensor (TIRS) data were employed. For classification, reflective bands with 30-meter spatial resolution were utilized. Specifically, bands 2, 3, 4, 5, 6, and 7 from Landsat 5 TM, and bands 2, 3, 4, 5, 6, and 7 from Landsat 8 OLI (corresponding to Blue, Green, Red, NIR, SWIR1, and SWIR2) were selected to leverage spectral information across the visible, near-infrared, and shortwave infrared regions for optimal land cover discrimination. Atmospheric correction of the satellite images was performed using the Fast Line of Sight Atmospheric Analysis of Spectral Hypercubes (FLAASH) method in the ENVI 5.3 software environment to eliminate atmospheric effects, such as absorption and scattering of electromagnetic waves (Rozenstein & Karnieli, 2011; Hussain et al., 2022). For land use classification, training samples were collected through field surveys and Google Earth for each land use type, with a minimum of 50 samples per land use type. To improve discrimination between agricultural types (rainfed, irrigated, orchard) which have similar spectral signatures in a single date, a multitemporal approach was employed. For each target year (1991, 2006, 2021), two cloud-free Landsat scenes were utilized: one during the peak of the growing season (e.g., May-June) and another during a different phenological stage (e.g., late summer/early autumn). This allowed the SVM classifier to leverage differences in crop phenology and moisture content. The training samples were collected from both dates to reflect these temporal characteristics. Additionally, the samples were carefully selected to ensure a well-distributed spatial coverage across the study area, providing a comprehensive representation of the landscape's variability and enhancing the accuracy of the classification process.

To ensure robust accuracy assessment, the collected reference samples for each year were randomly divided into two independent sets: 70% for training the SVM classifier and 30% for validation. This separation

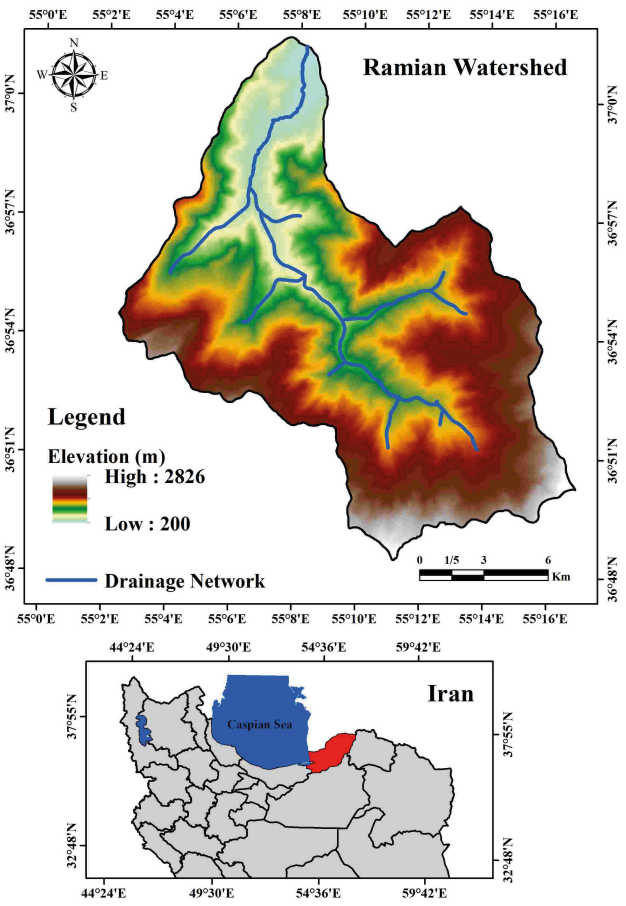

Fig. 1. Location and digital elevation model of the Ramian Watershed

guarantees that the accuracy metrics (Kappa and Overall Accuracy) are derived from data not used in model calibration, providing an unbiased evaluation of map performance.

To aid in visual interpretation and training sample selection, standard false-color composites (e.g., SWIR1-NIR-Red for Landsat 5/8) were generated to enhance the discrimination of vegetation, built-up areas, and bare soil. Training samples for the years 1991 and 2006 were also collected at unchanged points by comparing the satellite images of the target years and examining Google Earth images (Joorabian Shooshtari et al., 2015).

Collecting training labels for 1991 posed a challenge due to the lack of very high-resolution historical imagery (e.g., Google Earth) for that period. To address this, we adopted a post-classification comparison and temporal extrapolation strategy informed by local knowledge and ancillary data:

First, training samples for the 2006 and 2021 maps were directly collected using a combination of field surveys (2021) and interpretation of available high-resolution Google Earth imagery and Landsat time-series.

For 1991, we identified "unchanged areas" by analyzing multi-temporal Landsat composites (1991, 2006, 2021) and applying a robust change detection threshold based on spectral indices (e.g., NDVI) to locate pixels with a high probability of no land cover change between 1991 and 2006.

Training labels for these stable pixels in 1991 were then assigned the same class as their corresponding, spectrally similar, and visually confirmed pixels in the 2006 imagery. This approach relies on the premise that areas exhibiting minimal spectral change over a 15-year period in a predominantly forested watershed are likely to have retained the same land cover class.

Additionally, for areas suspected of change (e.g., new residential zones), labels were inferred from historical topographic maps, regional land-use studies from the era, and consultation with long-term local residents to augment and validate the sample selection. This multi-source approach mitigates the limitation posed by the absence of direct very high-resolution imagery for 1991.

Following the collection of training samples, the satellite images were classified using the supervised Support Vector Machine (SVM) method (Jiang et al., 2015). To account for potential spectral differences between the Landsat 5 TM (1991, 2006) and Landsat 8 OLI (2021) sensors and to ensure optimal classification accuracy for each unique temporal snapshot, separate SVM models were independently trained and calibrated for each of the three target years (1991, 2006, and 2021). This year-specific modeling approach mitigates inter-sensor variability and temporal changes in phenology or atmospheric conditions, ensuring that each classification reflects the spectral characteristics of its respective date.

Six land use categories were identified in the Ramian watershed: forest, rangeland, rainfed agriculture, irrigated agriculture, orchard, and residential areas. Given the background of previous studies conducted in the Hyrcanian forests, the similarity in land-use change patterns in the studied areas, and the relatively high accuracy of the SVM method in land-use classification, the present research also employs this method (Zabihi et al., 2020). The Radial Basis Function (RBF) kernel was used, and the Penalty Factor and Gamma parameters in the kernel function were set to 228 and 0.134, respectively. The accuracy of the classified map was assessed by comparing ground truth points with the classified map using the Kappa coefficient and Overall Accuracy (Hussain et al., 2020).

Landscape metrics calculation and screening

Landscape metrics are divided into three levels: patch (individual patches), class (all patches of the same land use), and landscape (all patches and classes within the land area). Analyzing these metrics at the class and landscape levels provide valuable indications into development patterns, diversity, and the distribution of various land use types in land use maps (Arekhi & Komaki, 2015; Abdolalizadeh et al., 2019).

In this study, we calculated a comprehensive set of metrics, including Class Area (CA), Number of Patches (NP), Percentage of Landscape (PLAND), Largest Patch Index (LPI), Patch Density (PD), Edge Density (ED), Landscape Shape Index (LSI), Interspersion and Juxtaposition Index (IJI), Patch Cohesion Index (COHESION), and Shannon's Diversity Index (SHDI), among others (see Tab. 1 and Tab. 2 for full list). Landscape metrics These metrics, associated with the geometry, shape, and configuration of patches, play a crucial role in defining landscape composition and spatial pattern (McGarigal & Marks, 1995).

In the present study, the Ramian watershed in Golestan province was selected as the spatial extent, and the spatial scale was determined based on the size of the Landsat satellite imagery cells, which is 30 meters. According to the land use maps for the years 1991, 2006, and 2021, two time periods, 1991 to 2006 and 2006 to 2021, were chosen according the temporal scale for investigating landscape metrics in the study area. To examine the changes and calculate landscape metrics in the Ramian watershed in Golestan province, Fragstats software and the 8-Cell Neighborhood Rule method with the No Sampling strategy were employed (McGarigal et al., 2002; Mostafazadeh & Talebi Khiavi, 2022). The 8-cell neighborhood rule considers diagonal pixel connections, providing a more realistic representation of landscape connectivity in fragmented or complex areas such as Hyrcanian forests. Moreover, the 8-cell method better captures patch shapes, edge effects, and ecological processes. Aligned with the research objectives, an extensive array of landscape metrics was computed for the years 1991, 2006, and 2021, spanning the spatial scale of the watershed. Comparisons then were made at both Class and Landscape levels, with the specifics outlined in the subsequent sections (Tab. 1 and Tab. 2). During the study period in the Ramian watershed of Golestan province, the preparation of land use maps and the calculation of landscape metrics were carried out, followed by the analysis and comparison of the changes. The graphical representation plots were created using the R programming language and were subsequently analyzed (R Core Team, 2021; Nordmann et al., 2022).

The selection of the 17 landscape metrics was guided by a comprehensive rationale aimed at capturing the multifaceted structural changes induced by agricultural and residential expansion in the Ramian watershed. Metrics were chosen to represent three complementary dimensions of landscape ecology: (1) Composition and Dominance (e.g., PLAND, CA, LPI) to quantify the area and dominance shifts between natural (forest, rangeland) and anthropogenic land uses; (2) Spatial Configuration and Fragmentation (e.g., NP, PD, DIVISION, SPLIT, MESH) to measure the degree of landscape subdivision, patch isolation, and habitat fragmentation critical for biodiversity; and (3) Shape Complexity and Connectivity (e.g., ED, LSI, PARA_AM, IJI, COHESION) to assess changes in patch geometry, edge effects, and the functional connectivity of the landscape matrix. This multi-dimensional

Tab. 1. List of selected landscape metrics at the Class level

Landscape metric	**Equation**	**Desciption**	**Unit**
Class Area	$CA = \sum_{j=1}^{n} a_{ij}\left(\frac{1}{10000}\right)$	The total area of land use patches (aij) represents the numerical domain, which is larger than one.	ha
Area-Weighted Mean Patch Area	$AREA_AM = \sum_{j=1}^{n} X_{ij}\left(\frac{a_{ij}}{\sum_{j=1}^{n} a_{ij}}\right)$	AREA_AM (area-weighted mean) is obtained by summing the patch metric value multiplied by the proportional abundance of each patch type, calculated as the patch area divided by the total sum of patch areas.	ha
Number of Patch	$NP = n_i$	n_i represents the count of patches belonging to patch type (class) i within the landscape.	(-)
Percentage of Landscape	$PLAND = P_i = \frac{\sum_{j=1}^{n} a_{ij}}{A}(100)$	P_i denotes the fraction of the landscape that patch type (class) i covers. a_{ij} represents the area (m^2) of patch ij, and A is the total landscape area (m^2).	%
Largest Patch Index	$LPI = \frac{\sum_{j=1}^{n} \max(a_{ij})}{A}(100)$	a_{ij} represents the area (m) of patch ij, while A denotes the total landscape area (m^2).	%
Patch Density	$PD = \frac{n_i}{A}(10000)(100)$	n_i refers to the count of patches in the landscape for patch type (class) i. A represents the total landscape area (m^2).	Number per hectare
Edge Density	$ED = \frac{\sum_{k=1}^{m} e_{ik}}{A}(10000)$	e_{ik} is the total length (m) of the edge in the landscape involving patch type (class) i, including both the landscape boundary and background segments related to patch type i. A represents the total landscape area (m^2).	Meter per hectare
Total Edge	$TE = \sum_{k=1}^{m} e_{ik}$	e_{ik} represents the overall length (m) of the edge in the landscape associated with patch type (class) i, encompassing both the landscape boundary and background segments related to patch type i.	Meters
Perimeter-Area Ratio_ Area-Weighted Mean	$PARA_{AM} = \text{Area weighted}(PARA\,patch_{ij})$	As a shape metric, summarizes each class as the area-weighted mean of its patches, which describes patch complexity but is not scale-independent, changing with variations in patch size while maintaining the same form.	(-)
Landscape Shape Index	$LSI = \frac{0.25 \sum_{k=1}^{m} e_{ik}^{*}}{\sqrt{A}}$	e_{ik}* denotes the total edge length (m) between patch types * (classes) i and k in the landscape, covering the entire landscape boundary and some or all background edge segments related to class i. A indicates the total landscape area (m^2).	(-)
Interspersion Juxtaposition Index	$IJI = \frac{-\sum_{k=1}^{m}\left[\frac{e_{ik}}{\sum_{k=1}^{m} e_{ik}} \ln\left(\frac{e_{ik}}{\sum_{k=1}^{m} e_{ik}}\right)\right]}{\ln(m-1)}$	e_{ik} is the overall edge length (m) between patch types (classes) i and k in the landscape, with m indicating the total number of patch types (classes) in the landscape, including the landscape border if present.	%
Patch Cohesion Index	$COHESION = \left[1 - \frac{\sum_{j=1}^{n} p_{ij}^{*}}{\sum_{j=1}^{n} p_{ij}^{*}\sqrt{a_{ij}^{*}}}\right]\left[1 - \frac{1}{\sqrt{Z}}\right]^{-1}(100)$	Perimeter (p_{ij}*) refers to the boundary length of patch ij measured in terms of the number of cell surfaces, and area (a_{ij}*) represents the patch ij‘s area measured in terms of the number of cells. Z denotes the total number of cells in the landscape.	(-)
Landscape Division Index	$DIVISION = \left[1 - \sum_{j=1}^{n}\left(\frac{a_{ij}}{A}\right)^2\right]$	a_{ij} represents the area (in square meters) of patch ij, and A denotes the total landscape area (in square meters).	Proportion
Contiguity Index_ Area-Weighted Mean	$CONTIG_{AM} = \text{mean}(CONTIG\,Patch_{ij})$	Representing the spatial connectedness or contiguity of patches within a landscape, describing their shape.	(-)
Effective Mesh Size	$MESH = \frac{\sum_{j=1}^{n} {a_{ij}}^2}{A}\left[\frac{1}{10000}\right]$	The variable a_{ij} represents the area (m^2) of patch ij, while A denotes the total landscape area (m_2).	ha
Splitting Index	$SPLIT = \frac{A^2}{\sum_{j=1}^{n} a_{ij}^2}$	a_{ij} stands for the area (m_2) of patch ij, and A represents the total landscape area (m_2).	(-)

Tab. 2. List of selected landscape metrics at the Landscape level

Landscape metric	Equation	Description	Unit
Largest Patch Index	$LPI = \frac{\max(a_{ij})}{A}(100)$	The area (m^2) of patch ij is denoted by aij, and A represents the total landscape area (m^2).	(%)
Total Edge	$TE = E$	E represents the total length (m) of the edge in the landscape.	Meters
Interspersion and Juxtaposition Index	$IJI = \frac{-\sum_{i=1}^{m}\sum_{k=i+1}^{m}\left[\left(\frac{e_{ik}}{E}\right)\ln\left(\frac{e_{ik}}{E}\right)\right]}{\ln(0.5[m(m-1)])}(100)$	e_{ik} is the total edge length (m) connecting patch types (classes) i and k in the landscape. E represents the overall edge length (m) in the landscape, excluding background. m is the number of patch types (classes) in the landscape, including the landscape border if present.	(%)
Patch Cohesion Index	$COHESION = \left[1 - \frac{\sum_{j=1}^{n} P_{ij}^{*}}{\sum_{j=1}^{n} P_{ij}^{*}\sqrt{a_{ij}^{*}}}\right]\left[1 - \frac{1}{\sqrt{Z}}\right]^{-1}(100)$	Perimeter (p_{ij}*) is the boundary length of patch ij measured in terms of the number of cell surfaces, and area (a_{ij}*) represents the area of patch ij measured in terms of the number of cells. Z denotes the total number of cells in the landscape.	(-)
Landscape Division Index	$DIVISION = \left[1 - \sum_{j=1}^{n}\left(\frac{a_{ij}}{A}\right)^2\right]$	Area (a_{ij}) refers to the patch ij's area measured in square meters, and A represents the total landscape area in square meters.	Proportion
Splitting Index	$SPLIT = \frac{A^2}{\sum_{i=1}^{m}\sum_{j=1}^{n} a_{ij}^2}$	Area (a_{ij}) refers to the patch ij's area measured in square meters, and A represents the total landscape area in square meters.	(-)
SHDI	$SHDI = -\sum_{i=1}^{m}(P * \ln P_i)$	Pi = proportion of the landscape occupied by patch type (class) i.	(-)

approach, aligning with established frameworks (McGarigal et al., 2002), ensures that the analysis moves beyond simple area changes to reveal the underlying spatial processes (such as fragmentation, increased edge contrast, and altered patch dispersion) that drive ecological degradation in human-influenced forested watersheds.

Analytical Tools and Software Platforms

The methodological framework was implemented using a combination of specialized software and programming platforms to ensure robust spatial analysis and metric computation. Landsat image preprocessing, atmospheric correction (FLAASH), and land use classification via the Support Vector Machine (SVM) algorithm were conducted in ENVI (version 5.3). The classified land use maps were then exported to FRAGSTATS (version 4.2), which served as the core computational engine for calculating the 17 selected landscape metrics at both class and landscape levels, employing the eight-cell neighborhood rule. To manage, integrate, and visualize spatial datasets, ArcGIS (version 10.8) was used extensively. Furthermore, all subsequent statistical analyses, generation of graphical outputs (including the violin plots), and synthesis of results were performed using the R programming language (R Core Team, 2021) within the RStudio integrated development environment.

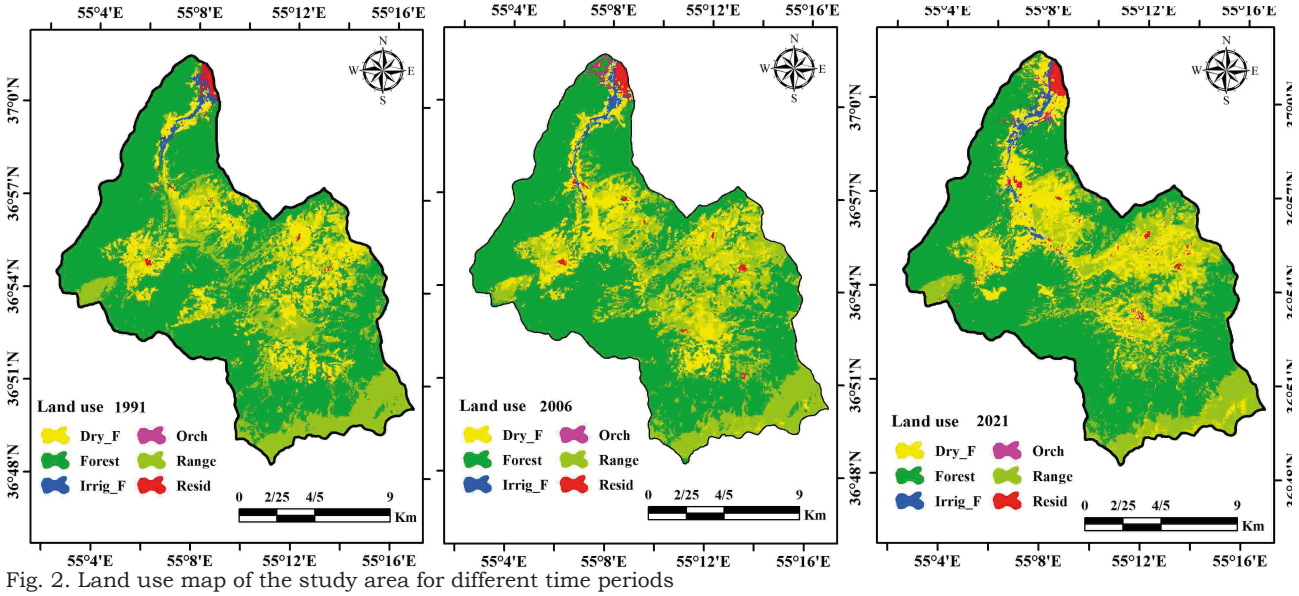

Fig. 2. Land use map of the study area for different time periods

3 RESULTS

Land use changes over time

Figure 2 shows the land use map of the study area across different time periods. The evaluation of the prepared land use maps for the watershed area revealed Kappa coefficients of 0.74, 0.79, and 0.87 for the years 1991, 2006, and 2021, respectively. Additionally, the Overall Accuracy of the generated maps was computed as 81%, 86%, and 91% for the corresponding years. The temporal increase in classification accuracy can be explained by two key factors: (1) technological advances in satellite sensors (from Landsat 5 to Landsat 8/9), which improved spectral discrimination between land cover classes, and (2) the greater availability and precision of ground reference data for the recent period (2021) compared to the historical baseline (1991).

Changes in landscape metrics across land uses

The comparison of landscape metrics at the class level is presented in Figure 3, while Fig. 4 shows the changes in landscape metrics over the study years.

As shown in Figure 3, AREA_AM and CA (patch area) exhibit notable differences, particularly for Forest and Rangelands, while ED (edge density) shows moderate variations, reflecting changes in patch boundaries. Beyond these, several other key trends are evident. The Interspersion Juxtaposition Index (IJI) increased substantially for Dry Farming and Forest, suggesting a greater intermixing of these classes with others. Concurrently, the Landscape Shape Index (LSI) rose for most anthropogenic classes (e.g., Dry Farming, Residential), indicating more irregular and complex patch shapes. Furthermore, a divergent fragmentation process is highlighted by the Number of Patches (NP), which decreased for natural classes (Forest, Rangeland) but increased for agricultural and residential uses.

Changes in landscape-level landscape metrics across different years

To assess the overall structural dynamics of the watershed, landscape-level metrics were analyzed. Figure 4 illustrates the statistical distribution of key metrics across the three study years, where each data point represents the single, watershed-scale value for that metric and year.

Similarly, Figure 5 tracks the temporal trend of these watershed-level values over the 30-year period.

According to Figure 4, the CA and PLAND landscape metrics have not changed significantly over the study period. Meanwhile, the values of other landscape metrics increased in the mid-year but declined in the recent period in the study area.

Temporal trends in landscape metrics

Figure 5 tracks the temporal trend of these watershed-level values over the 30-year period.

Over the 30-year study period, key metrics reveal a restructuring of the landscape. The total number of patches (NP) at the landscape level decreased

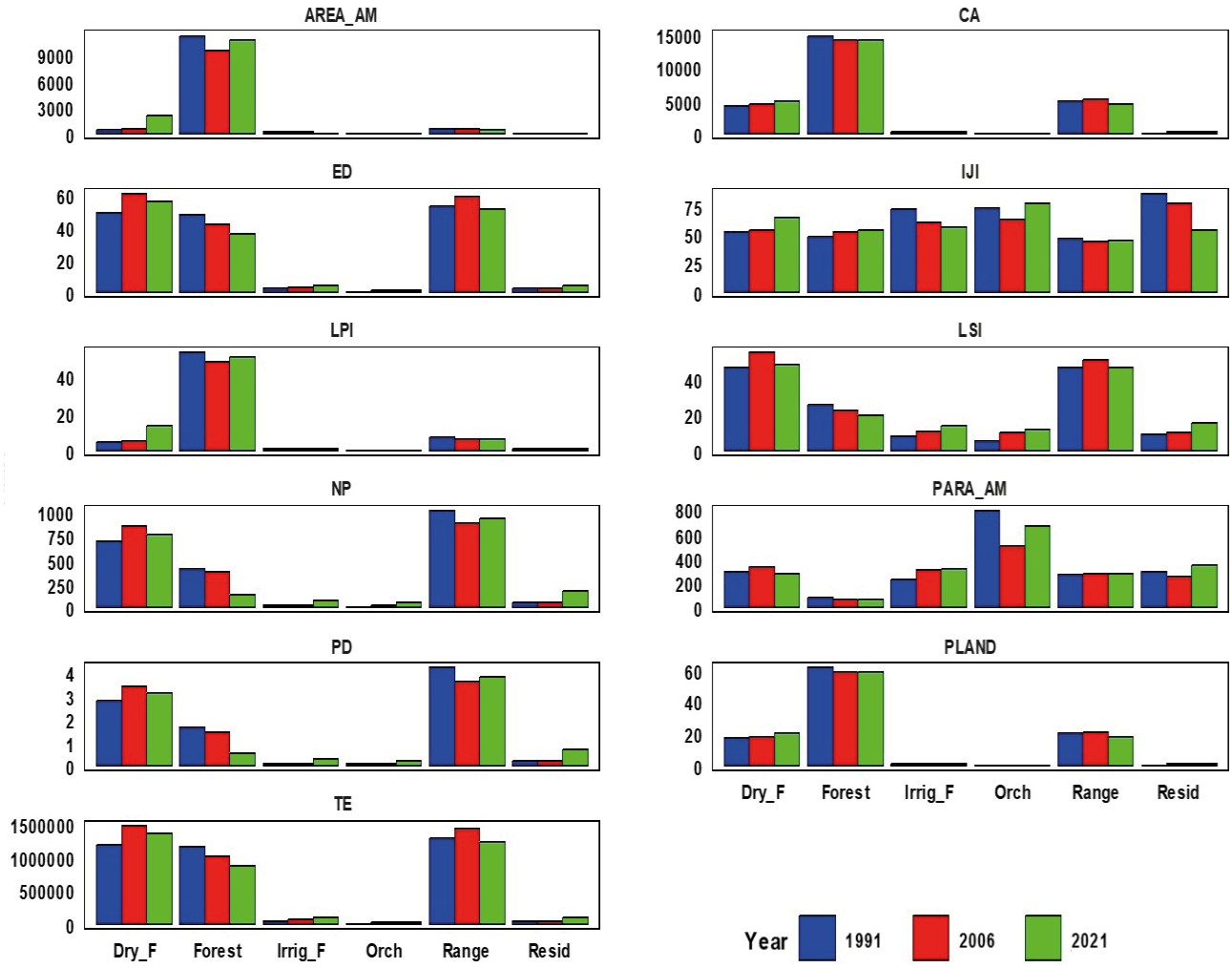

Fig. 3. Variation of landscape metrics across different land uses at the class level over the studied years (Dry_F: Dry farming, Forest: Forest, Irrig_F: Irrigated farming, Orch: Orchard, Range: Rangeland, Resid: Residential)

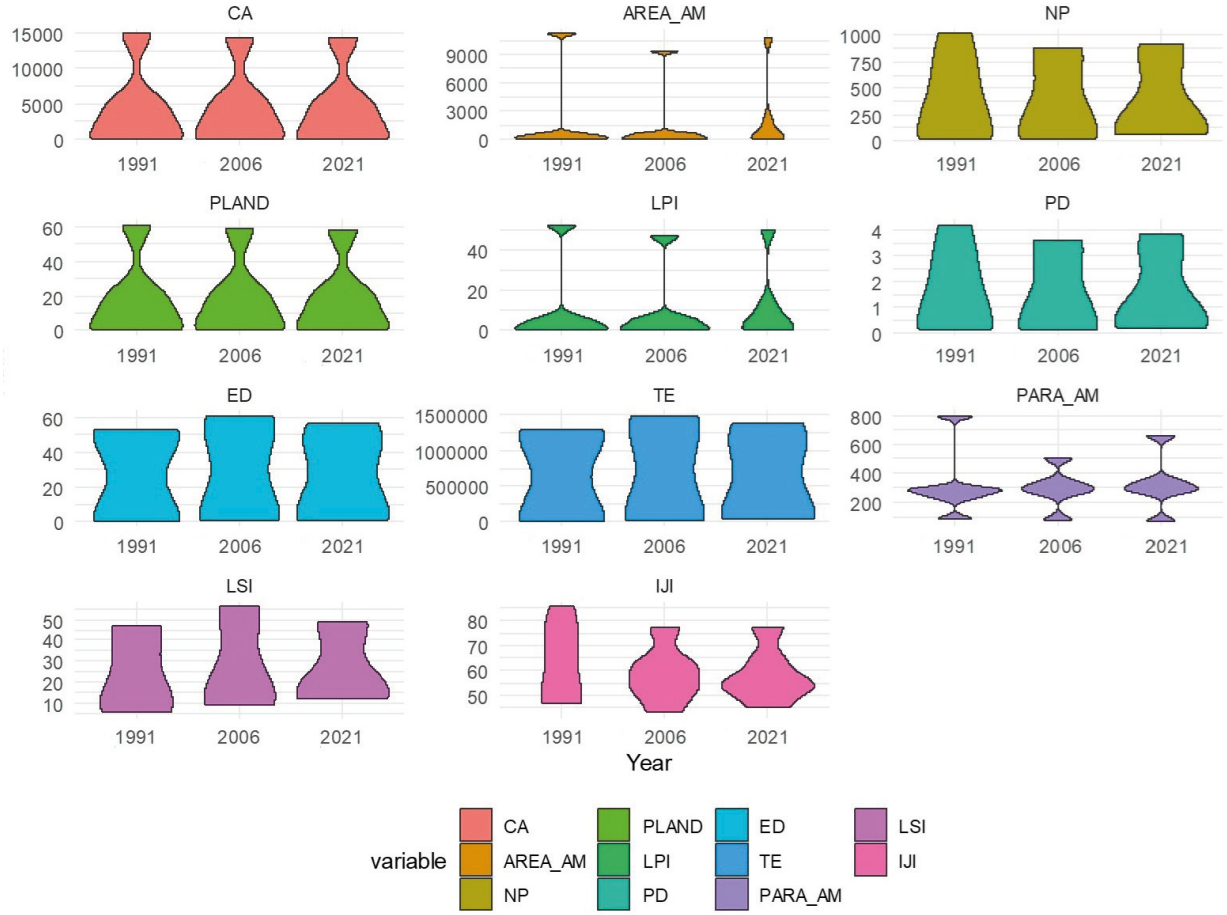

Fig. 4. Violin plot of landscape-level landscape metrics over different years in the study area (CA: Class Area, AREA_AM: Area-Weighted Mean Patch Area, NP: Number of Patches, PLAND: Percentage of Landscape, LPI: Largest Patch Index, PD: Patch Density, ED: Edge Density, TE: Total Edge, PARA_AM: Area-Weighted Mean Perimeter-Area Ratio, LSI: Landscape Shape Index, IJI: Interspersion Juxtaposition Index)

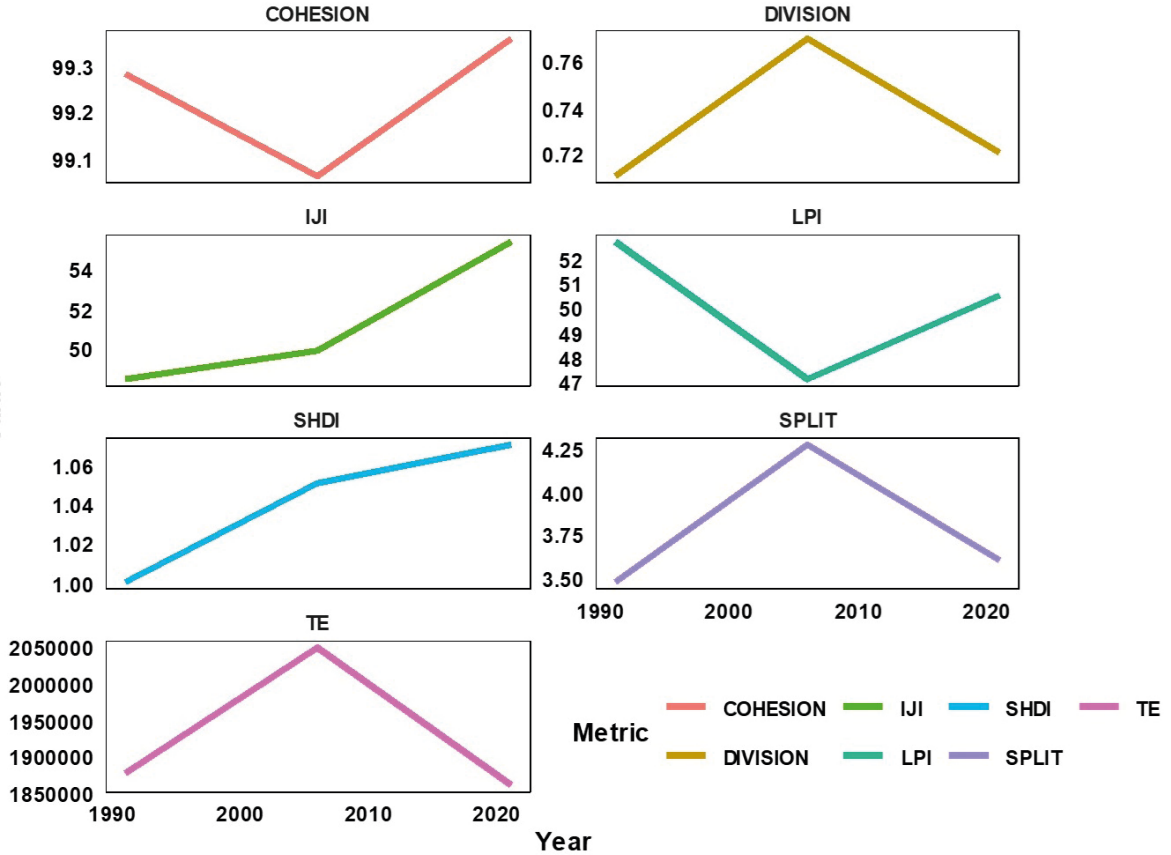

Fig. 5. Variation of landscape metrics at class level over the studied years

from 2204 in 1991 to 2132 in 2021, suggesting a net consolidation of patches. However, this overall decrease masks a contrasting trend at the class level, where NP increased for expanding anthropogenic land uses such as dry farming and residential areas (see Section 4.2), indicating fragmentation within these specific categories. Concurrently, the Largest Patch Index (LPI) declined from 52.67% to 50.48%, reflecting a reduced dominance of the largest patch. Patch Density (PD) also showed a consistent decrease from 9.03 to 8.73 per hectare. Furthermore, Total Edge (TE) exhibited a non-linear trend, ultimately decreasing from 1,874,370 meters to 1,858,650 meters. These combined trends (net patch consolidation alongside reduced dominance of the largest patch and edge density) point towards a complex process of landscape division and reorganization in the Ramian watershed.

4 DISCUSSION

Land use changes over time

Table 3 illustrates land use changes in the study area over the years 1991, 2006, and 2021.

The land use transition matrix (Tab. 3) reveals a clear and consequential shift in the Ramian watershed over three decades. The most striking transformation is the large-scale conversion of natural lands to agriculture, particularly to rainfed farming, which expanded by 29.98 km² (154.5%). This expansion directly correlates with the decline in forest (-6.71 km²) and rangeland (-4.45 km²) cover, underscoring agricultural encroachment as the primary driver of land use change in this forest-dominant landscape. Concurrently, the more than twofold increase in residential area signals growing urbanization pressure. These parallel trends of agricultural expansion and settlement growth collectively point to intensified anthropogenic pressure, setting the stage for the significant alterations in landscape structure quantified in the following sections.

Our primary objective was to assess the structural and configurational consequences of land-use change on the watershed's landscape, rather than to model the precise transition pathways between land-use classes. Therefore, the analytical framework was deliberately centered on a suite of landscape metrics that quantify patterns of fragmentation, connectivity, shape complexity, and diversity. This approach allows us to diagnose the ecological footprint of aggregate land-use changes (specifically, the net loss of natural covers and expansion of anthropogenic uses) and its implications for landscape integrity, moving beyond accounting of „from-to" conversions to understand their spatial-structural outcomes.

Landscape metrics variations across land uses

Analysis of class-level metrics (Fig. 3) reveals distinct and divergent trends between natural and human-made land uses over the 30-year period.

Composition and Dominance: Natural land uses (Forest and Rangeland) declined in both total area (PLAND: Forest 61.06% to 58.31%; Rangeland 20.56% to 18.74%) and mean patch size (AREA_AM). Conversely, anthropogenic uses expanded significantly, with Dry farming, Residential, and Orchard areas increasing by factors of 1.19, 2.07, and 6.70, respectively. The Largest Patch Index (LPI) increased substantially for residential (by 135%), orchard (by 498%), and dry farming (by 311%) land uses over the 30 years. In contrast, the LPI for forest, irrigated farming, and rangeland decreased slightly (by 5%, 2%, and 15%, respectively).

Fragmentation and Configuration: Patch Density (PD) increased for all human-made land uses (most sharply in Irrigated farming: +411%), signaling heightened fragmentation. In contrast, Forest and Rangeland showed decreased PD, suggesting patch aggregation or loss. The Number of Patches (NP) followed a similar pattern, decreasing for natural covers but increasing for anthropogenic ones.

Shape and Edge Complexity: Edge Density (ED) and Total Edge (TE) increased for Dry farming, Irrigated farming, and Residential areas, indicating more irregular, dispersed, and complex patch shapes. Forest and Rangeland exhibited decreasing ED/TE, reflecting simplification and regularization of their remaining patches. The Perimeter-Area Ratio (PARA_AM) and Landscape Shape Index (LSI) increased for most land uses, pointing to overall growing shape complexity, although Dry farming and Orchards showed a trend towards more regular geometries over time.

Spatial Arrangement: The Interspersion and Juxtaposition Index (IJI) increased for Dry farming, Forest, and Orchards, denoting greater intermixing with other land cover types. IJI decreased for Irrigated farming, Rangeland, and Residential areas, suggesting these types became more clustered and less adjacent to other classes.

In summary, the metrics collectively depict a landscape transformation where expanding human-made land uses become more dominant, fragmented, and geometrically complex, while contracting natural land uses lose area, become more aggregated, and exhibit simplified shapes.

Changes in landscape-level landscape metrics across years

Violin plots of landscape-level metrics (Fig. 4) highlight key temporal dynamics in landscape structure. The widening distributions of Class Area (CA) and Area-Weighted Mean Patch Area (AREA_AM) over time point to increasing heterogeneity in patch sizes across the landscape. Patch configuration metrics (NP, PD) exhibited marked fluctuations, with a noticeable dip in 2006, whereas composition metrics (PLAND, LPI) remained relatively stable. Edge-related metrics (ED, TE) showed minimal change over the period. Shape complexity displayed divergent trends: PARA_AM varied significantly between years, while LSI was more consistent. The substantial inter-annual variation in the Interspersion Juxtaposition Index (IJI) reflects dynamic shifts in the spatial mixing of land cover types.

Temporal trends in landscape metrics

According to Figure 5, The IJI at the landscape level exhibited an increasing trend, rising from 48.44% in 1991 to 55.35% in 2021. The COHESION index also showed a greatly upward trend, likely due to the limited number of land use categories in the study area, increasing from 99.27 in 1991 to 99.35 in 2021. Similarly, the DIVISION index, which reflects landscape

Tab. 3. Land use distribution in the Ramian area for the years 1991, 2006, and 2021

Year	Dry farming	Forest	Irrigated agriculture	Orchard	Rangeland	Residential
1991	41.19	149.02	2.01	0.08	50.19	1.54
2006	43.81	143.48	2.11	0.58	51.94	2.12
2021	49.39	142.31	2.86	0.53	45.74	3.19

fragmentation, increased from 0.712 in 1991 to 0.721 in 2021. However, its trajectory differed across the study period, with an initial rise from 1991 to 2006, followed by a decline from 2006 to 2021. The results indicate that the CONTIG_AM value remained relatively stable over the study period, measuring 0.8711 in 1991 and 0.872 in 20021, with a slight dip to 0.8593 in 2006. The MESH index in the Ramian watershed decreased in the first period (1991-2006) and increased in the second period (2006-2021). While the overall trend of MESH value slightly declined from 7024.1 in 1991 to 6786.3 hectares in 2021, a closer examination reveals a significant increase due to dry farming and residential land uses expansion over the 30-year research period. The SPLIT index showed an increasing trend during the first period rising from 3.47 in 1991 to 4.26 in 2006, followed by a decreasing trend from 2006 to 2021. However, over the entire study period, the SPLIT value increased from 3.47 to 3.59, indicating greater fragmentation of land uses in the Ramian watershed. The SHDI value, representing landscape diversity, increased from 1 in 1991 to 1.04 in 2006 and 1.07 in 2021, showcasing a rising trend in landscape heterogeneity. Similarly, the SIDI value increased from 0.556 in 1991 to 0.583 in 2021, further indicating an increase in land use diversity over time.

In Ramian, there is a notable simultaneous decline in forest/rangeland AREA_AM and an increase in dry farming PARA_AM (from 270.63 to 290.24), reflecting patch regularization, which contrasts with the irregular fragmentation observed by Kumar et al. (2018) in Indian forests. While urban-driven fragmentation was noted by Bihamta Toosi et al. (2014) and Dezhkam and Jabbarian Amiri (2015) in Iran, this study highlights agricultural encroachment, particularly the expansion of rainfed farming by 29.98 km², as the primary driver of change in Ramian, distinguishing it from urban-focused trends elsewhere. The 6.71 km² loss of forest aligns with Zabihi et al. (2020) findings in Iran, but contrasts with Cervelli et al. (2025)'s Mediterranean focus on built-up expansion. Unlike Yang et al. (2025) linear urban growth, Ramian's metrics (e.g., NP, TE) show non-linear trends, with fragmentation peaking in 2006 and later stabilizing, suggesting localized policy impacts or ecological thresholds. The IJI increase (48.44% to 55.35%) reflects unique shifts in adjacency, differing from De Barros Ferraz et al. (2005) connectivity loss, emphasizing Ramian's mixed-use transitions. This study applied a multi-metric temporal analysis (11 indices), similar to Cervelli et al. (2025), with violin plots (Fig. 4) illustrating interannual metric volatility, as seen in Deng et al. (2009) work on landscape fragmentation indices. The 20.24% expansion of rainfed farming, in contrast to Yang et al. (2025) findings of cropland decline, highlights the need for localized agricultural zoning.

The stable COHESION index at the landscape level (99.27 to 99.35) should not be interpreted as a sign of ecological resilience. This landscape-level metric aggregates the connectivity of all patch types, and its stability likely results from counterbalancing trends: a probable decrease in connectivity within natural land-use patches (forest and rangeland) may have been offset by an increase in connectivity within expanding anthropogenic patches (e.g., dry farming). Consequently, this stability reflects a structural homogenization at the landscape level where the connectivity of human-dominated matrices replaces that of natural habitats, rather than indicating the persistence of ecological connectivity crucial for biodiversity. Future studies should analyze class-level cohesion for aggregated natural and anthropogenic groups to test this hypothesis. This research offers a unique quantification of agriculture-driven fragmentation in semi-arid watersheds, redefining fragmentation paradigms in mixed-use landscapes through the juxtaposition of regularization (dry farming) and irregularity (residential PARA_AM).

The observed land-use changes are direct manifestations of underlying socio-economic drivers. The dramatic expansion of rainfed agriculture is the principal force behind forest fragmentation. The associated increases in Edge Density (ED) and Landscape Shape Index (LSI) for this class indicate a pattern of small-scale, irregular encroachment into natural forests, likely driven by local livelihood needs and agricultural extensification policies on marginal lands. This process directly erodes core forest habitat, as evidenced by the decline in the forest's Largest Patch Index (LPI). The non-linear trend in fragmentation metrics (peaking around 2006 before partially stabilizing) suggests a complex interplay of driving forces. The initial rise may be linked to post-war population growth and intensive land conversion. The subsequent moderation could reflect the delayed impact of national conservation policies for the Hyrcanian forests or a saturation effect where the most accessible lands were already converted. This pattern underscores that landscape outcomes result from the tension between development pressures and conservation responses over time.

Perspectives

To address these challenges, future research should explore the drivers of land use changes, indicating socio-economic factors, policy shifts, climate variations. Investigating the ecological consequences of these transformations, such as their impacts on biodiversity, ecosystem services, and hydrological processes, will provide a more holistic understanding of long-term landscape dynamics. Integrating ecological models with landscape metrics could help predict future changes and support informed land management decisions.

Drivers of Landscape Change

Landscape changes are driven by complex socio-economic and policy factors. The significant growth of rainfed agriculture (29.98 km²) in this study is linked to regional agricultural policies and population growth. Government subsidies for dryland farming, coupled with the rising demand for food and livelihoods, likely led to the conversion of forests and rangelands into cultivated areas. This is reflected in increased NP, PD, and ED for agricultural land. The expansion of residential areas, though smaller, indicates rural settlement growth and weak enforcement of land-use regulations, contributing to greater irregularity (PARA_AM) and dispersion (IJI) of anthropogenic patches. Non-linear trends in NP and SPLIT around 2006 may reflect shifts in agricultural policy or economic factors. While a deeper socio-economic analysis was beyond the scope, recognizing these drivers is essential for understanding landscape changes and informing management strategies.

Management implications and environmental impacts

The marked increase in fragmentation metrics (e.g., NP, PD) and the decline in forest integrity signal a tangible decline in ecosystem services, loss of biodiversity, and heightened vulnerability to hazards such as erosion and flooding. To counter this trend, three key management actions are recommended: 1) enforcing stricter land-use change policies prioritizing the conservation of the remaining large forest patches (high LPI), 2) promoting sustainable and consolidated

agricultural practices within existing farmlands instead of expanding new frontiers to reduce edge effects and shape complexity (ED and LSI), and 3) establishing and restoring ecological corridors between remaining forest patches to enhance landscape connectivity (COHESION) and mitigate the negative impacts of habitat isolation. Regular monitoring of these landscape metrics can serve as an effective tool for evaluating the efficacy of these management policies in the future.

Study Limitations and Uncertainties

The accuracy of the landscape metric analysis depends on the classification accuracy of the land-use maps. Although the accuracy of classification is acceptable, misclassification, especially in mixed or transitional areas, adds uncertainty to the metrics, particularly for smaller patch classes. The selection of a single spatial resolution (30 m Landsat pixel) influences the sensitivity of metrics like PD and ED; a finer resolution might reveal finer-scale fragmentation patterns. While the selected metrics effectively describe structural changes, they are indirect proxies for ecological function (e.g., actual species movement or soil erosion processes). Finally, the analysis captures correlation in time but does not establish causal mechanisms; the identified landscape changes are linked to, but not conclusively proven to be driven by, the discussed socio-economic factors without dedicated driver analysis.

5 CONCLUSIONS

This study examined land use changes in the Ramian watershed over a 30-year period, utilizing landscape metrics at both class and landscape levels within a typical Hyrcanian forest under increasing human influence. The results show a rise in the number of patches at the landscape level, indicating fragmentation and the division of land uses, which is particularly significant for natural land uses. The decline in natural land areas and the expansion of human-made land uses are evident from the PLAND metric and the increasing number of patches. The LPI reveals a growing dominance of dry farming, residential areas, and orchards while, other land uses have declined. Human-made land uses (irrigated farming, residential areas, and dry farming) have become more irregular, scattered, and geometrically complex, as indicated by increasing ED values. In contrast, forest and rangeland land uses have experienced a decline in ED, reflecting a reduction in their structural integrity. The highest percentage change in landscape metrics at the landscape level was observed in the Interspersion and Juxtaposition Index (IJI) (14.36%), while at the class level, the most significant change was in the Mean Effective Mesh Size (MESH) (436%). Additionally, Edge Density (ED) increased by 0.83% at the landscape level and by 114% at the class level. Metrics such a s IJI, COHESION, DIVISION, and SHDI indicate that the Ramian watershed has undergone a degradative trend, characterized by reduced connectivity, increased dispersion, and greater irregularity in land use patches. This structural transformation proves the need for critical conservation measures/ activities to prevent further degradation of natural land uses, preserve ecological balance, and promote sustainable development. The results of this study emphasized the dynamic nature of land use changes in a forest-dominant watershed, revealing substantial transformations in both natural and human-made landscapes. In the upper reaches of the Ramian watershed, rangelands are being intensively utilized, while the middle sections are experiencing significant forest-to-rainfed agricultural land conversion. To curb further ecological degradation, the enforcement of robust conservation policies is crucial. In the lower watershed, fostering agroforestry practices can play a key role in boosting sustainability and maintaining ecological stability. Implementing these strategies, alongside comprehensive land use management, would safeguard the watershed's natural resources and help reduce the negative impacts of human-induced land use changes. The use of advanced remote sensing techniques, indicating the SVM algorithm and landscape metrics, has proven effective in assessing these shifts. The identified trends of landscape fragmentation, increasing complexity, and human-induced alterations stress the urgency of implementing proactive ecological restoration and sustainable land management strategies to mitigate further degradation and ensure long-term environmental health in similar forested watersheds.

REFERENCES

Abdolalizadeh, Z., Ebrahimi, A., & Mostafazadeh, R. (2019). Landscape pattern change in Marakan protected area, Iran. Regional Environmental Change, 19, 1683–1699. https://doi.org/10.1007/s10113-019-01504-9

Alaei, N., Mohammadzadeh, F., Mostafazadeh, R., & Talebi Khiavi, H. (2024). Assessing spatiotemporal urban green space per capita and its connectivity in a small size city in Northwest Iran. GeoJournal, 89(4), 148. https://doi.org/10.1007/s10708-024-11159-7

Alaei, N., Mostafazadeh, R., Esmali Ouri, A., Hazbavi, Z., Sharari, M., & Huang, G. (2022). Spatial Comparative Analysis of Landscape Fragmentation Metrics in a Watershed with Diverse Land Uses in Iran. Sustainability, 14(22), 14876. https://doi.org/10.3390/su142214876

Arekhi, S., & Komaki, B. (2015). Detecting and assessing desertification using landscape metrics in GIS environment (Case study: Ain-e-khosh Region, Iran). Environmental Resources Research, 3(2), 122–138. https://doi.org/10.22069/ijerr.2015.2709

Azareh, A., Rafiei Sardooi, E., & Mircholi, F. (2024). Analyzing and predicting the trend of land cover degradation and determining the changes in landscape metrics using remote sensing. Water and Soil Management and Modelling, 4(4), 15–32. https://doi.org/10.22098/mmws.2023.13021.1295

Baude, M., Meyer, B. C., & Schindewolf, M. (2019). Land use change in an agricultural landscape causing degradation of soil-based ecosystem services. Science of the Total Environment, 659, 1526–1536. https://doi.org/10.1016/j.scitotenv.2018.12.455

Bihamta Toosi, N., Safianian, A., & Fakheran, S. (2014). Analysis of land cover changes in the central part of Isfahan (Iran) using landscape metrics. Iranian Journal of Applied Ecology, 2(6), 77–88. http://dorl.net/dor/20.1001.1.24763128.1392.2.6.7.6

Blyth, E., Clark, D. B., Ellis, R., Huntingford, C., Los, S., Pryor, M., Best, M., & Sitch, S. (2011). A comprehensive set of benchmark tests for a land surface model of simultaneous fluxes of water and carbon at both the global and seasonal scale. Geoscientific Model Development, 4(2), 255–269. https://doi.org/10.5194/gmd-4-255-2011

Cervelli, E., di Perta, E. S., & Pindozzi, S. (2025). Diachronic analyses on land use changes and vernacular architecture distribution, to support

agricultural landscape development. Journal of Cultural Heritage, 71, 242–251. https://doi.org/10.1016/j.culher.2024.12.001

Climate-Data.org. (2025). Climate data: Golestan province, Iran. [Data set]. https://en.climate-data.org/asia/iran/golestan-2189/

da Silva, A. L., de Nunes, A. J. N., Marques, M. L., Ribeiro, A. Í., & Longo, R. M. (2021). Assessing the fragility of forest remnants by using landscape metrics. Comparison between river basins in Brazil and Portugal. Environmental Monitoring and Assessment, 193(4), 172. https://link.springer.com/article/10.1007/s10661-021-08953-y

Darvishi, A., Yousefi, M., Schirrmann, M., & Ewert, F. (2024). Exploring biodiversity patterns at the landscape scale by linking landscape energy and land use/land cover heterogeneity. Science of The Total Environment, 916, 170163. https://doi.org/10.1016/j.scitotenv.2024.170163

De Barros Ferraz, S. F., Vettorazzi, C. A., Theobald, D. M., & Ballester, M. V. R. (2005). Landscape dynamics of Amazonian deforestation between 1984 and 2002 in central Rondônia, Brazil: assessment and future scenarios. Forest Ecology and Management, 204(1), 69–85. https://doi.org/10.1016/j.foreco.2004.07.073

Deng, J. S., Wang, K., Hong, Y., & Qi, J. G. (2009). Spatio-temporal dynamics and evolution of land use change and landscape pattern in response to rapid urbanization. Landscape and urban planning, 92(3–4), 187–198. https://doi.org/10.1016/j.landurbplan.2009.05.001

Dezhkam, S. S., & Jabbarian Amiri, B. (2015). Monitoring the landscape changes using synoptic analysis and satellite images (Case study: Rasht township). Journal of Natural Environment, 68(2), 225–238. https://doi.org/10.22059/jne.2015.54950

Diuk-Wasser, M. A., VanAcker, M. C., & Fernandez, M. P. (2021). Impact of land use changes and habitat fragmentation on the eco-epidemiology of tick-borne diseases. Journal of Medical Entomology, 58(4), 1546–1564. https://doi.org/10.1093/jme/tjaa209

Forman, R. T. T. (2008). Urban regions: Ecology and planning beyond the city. Cambridge University Press. https://doi.org/10.1017/CBO9780511754982

Gustafson, E. J. (1998). Quantifying landscape spatial pattern: what is the state of the art? Ecosystems, 1(2), 143–156. https://doi.org/10.1007/s100219900011

Herold, M., Couclelis, H., & Clarke, K. C. (2005). The role of spatial metrics in the analysis and modeling of urban land use change. Journal of Computers, Environment and Urban Systems, 29, 369–399. https://doi.org/10.1016/j.compenvurbsys.2003.12.001

Hersperger, A. M., Oliveira, E., Pagliarin, S., Palka, G., Verburg, P., Bolliger, J., & Grădinaru, S. (2018). Urban land-use change: The role of strategic spatial planning. Global Environmental Change, 51, 32–42. https://doi.org/10.1016/j.gloenvcha.2018.05.001

Heydari-Guran, S., & Ghasidian, E. (2024). Ecological Landscape Structure and Game Management Strategy among the Upper Palaeolithic Societies of Southern Zagros Mountains. Environmental Archaeology, 29(3), 192–213. https://doi.org/10.1080/14614103.2021.1996889

Huggett, R. J., & Cheesman, J. (2002). Topography and the environment. Prentice Hall.

Hussain, S., Lu, L., Mubeen, M., Nasim, W., Karuppannan, S., Fahad, S., Tariq, A., Mousa, B. G., Mumtaz, F., & Aslam, M. (2022). Spatiotemporal variation in land use land cover in the response to local climate change using multispectral remote sensing data. Land, 11(5), 595. https://doi.org/10.3390/land11050595

Hussain, S., Mubeen. M, Akram, W., Ahmad, A., Habib-ur-Rahman, M., Ghaffar, A., Amin, A., Awais, M., Umar Farid, H., Farooq, A., & Nasim, W. (2020). Study of land cover/land use changes using RS and GIS: a case study of Multan district, Pakistan. Environmental Monitoring and Assessment, 192, no 2. https://doi.org/10.1007/s10661-019-7959-1

Chang, X., Zhang, F., Cong, K., & Liu, X. (2021). Scenario simulation of land use and land cover change in mining area. Scientific Reports, 11(1), 1–12. https://doi.org/10.1038/s41598-021-92299-5

Chiesa, D., Pelorosso, R., Leone, A., & Berger, U. (2009). Landscape dynamics in an abandoned rural area of the central Apennine Mountains. In G. Giametta, & G. Zimbalatti (Eds.), Technology and management to ensure sustainable agriculture, agro-systems, forestry and safety. Proceedings of the XXXIII CIOSTA - CIGR V Conference (pp. 1691–1696). Reggio Calabria: Editure Artemis. https://ulb-dok.uibk.ac.at/download/pdf/5698814.pdf

Jiang, W., Chen, Z., Lei, X., Jia, K., & Wu, Y. (2015). Simulating urban land use change by incorporating an autologistic regression model into a CLUE-S model. Journal of Geographical Sciences, 25(7), 836–850. https://doi.org/10.1007/s11442-015-1205-8

Joorabian Shooshtari, S., & Gholamalifard, M. (2015). Scenario-based land cover change modeling and its implications for landscape pattern analysis in the Neka Watershed, Iran. Remote Sensing Applications: Society and Environment, 1, 1–19. https://doi.org/10.1016/j.rsase.2015.05.001

Khan, M., & Chen, R. (2025). Assessing the Impact of Land Use and Land Cover Change on Environmental Parameters in Khyber Pakhtunkhwa, Pakistan: A Comprehensive Study and Future Projections. Remote Sensing, no. 170, 17(1). https://doi.org/10.3390/rs17010170

Kumar, M., Denis, D. M., Singh, S. K., Szabó, S., & Suryavanshi, S. (2018). Landscape metrics for assessment of land cover change and fragmentation of a heterogeneous watershed. Remote Sensing Applications: Society and Environment, 10, 224–233. https://doi.org/10.1016/j.rsase.2018.04.002

Lambin, E. F., Geist, H. J., & Lepers, E. (2003). Dynamics of land-use and land-cover change in tropical regions. Annual Review of Environment and Resources, 28(1), 205–241. https://doi.org/10.1146/annurev.energy.28.050302.105459

McGarigal, K. (2002). FRAGSTATS: Spatial Pattern Analysis Prog-ram for Categorical Maps. Computer software program produced by the authors at the University of Massachuse-tts, Amherst. http://www.umass.edu/landeco/research/fragstats/fragstats.html

McGarigal, K., & Marks, B. J. (1995). Spatial pattern analysis program for quantifying landscape structure. Gen. Tech. Rep. PNW-GTR-351. US Department of Agriculture, Forest Service, Pacific Northwest Research Station, 1–122. https://doi.org/10.2737/PNW-GTR-351

McLeod, A. M., Leroux, S., Little, C. L., Massol, F., Vander Wal, E., Wiersma, Y. F., Gounand, I., Loeuille, N., & Harvey, E. (2025). Quantifying elemental diversity to study landscape ecosystem function. Trends in Ecology & Evolution, 40(1), 57–66. https://doi.org/10.1016/j.tree.2024.09.007

Mirzaei, S., Esmali ouri, A., Mostafazadeh, R., Ghorbani,

A., & Mirzaei, S. (2018). Flood Hydrograph Simulation and Analysis of its Components with Landscape Metrics in Amoughin Watershed, Ardabil Province. Iranian Journal of Ecohydrology, 5(2), 357–372. https://doi.org/10.22059/ije.2018.231141.547

Mony, C., Vannier, N., Burel, F., Ernoult, A., & Vandenkoornhuyse, P. (2024). The root microlandscape of arbuscular mycorrhizal fungi. New Phytologist, 244(2), 394–406. https://doi.org/10.1111/nph.20048

Mostafazadeh, R., & Talebi Khiavi, H. (2022). Landscape change assessment and its prediction in a mountainous gradient with diverse land-uses. Environment, Development and Sustainability, 26, 3911–3941 https://doi.org/10.1007/s10668-022-02862-x

Nie, Y., Zhang, X., Yang, Y., Liu, Z., He, C., Chen, X., & Lu, T. (2023). Assessing the impacts of historical and future land-use/cover change on habitat quality in the urbanizing Lhasa River Basin on the Tibetan Plateau. Ecological Indicators, 148, 110147. https://doi.org/10.1016/j.ecolind.2023.110147

Nordmann, E., McAleer, P., Toivo, W., Paterson, H., & DeBruine, L. M. (2022). Data visualization using R for researchers who do not use R. Advances in Methods and Practices in Psychological Science, 5(2), 25152459221074654. https://doi.org/10.1177/25152459221074654

O'Neill, R. V., Krummel, J. R., Gardner, R. E. A., Sugihara, G., Jackson, B., DeAngelis, D. L., Milne, B. T., Turner, M. G., Zygmunt, B., Christensen, S. W., Dale, V. H., & Graham, R. L. (1988). Indices of landscape pattern. Landscape ecology, 1(3), 153–162. https://doi.org/10.1007/BF00162741

Ortiz-Colin, P., & Hulshof, C. M. (2024). Ecotones as windows into organismal-to-biome scale responses across neotropical forests. Plants, 13(17), 2396. https://doi.org/10.3390/plants13172396

Pickett, S. T., & Cadenasso, M. L. (1995). Landscape ecology: spatial heterogeneity in ecological systems. Science, 269(5222), 331–334. https://doi.org/10.1126/science.269.5222.331

R Core Team. (2021). R: A language and environment for statistical computing [Computer software]. R Foundation for Statistical Computing. https://www.R-project.org/

Rafiee, R., Mahiny, A. S., Khorasani, N., Darvishsefat, A. A., & Danekar, A. (2009). Simulating urban growth in Mashad City, Iran through the SLEUTH model (UGM). Cities, 26(1), 19–26. https://doi.org/10.1016/j.cities.2008.11.005

Rozenstein, O., & Karnieli, A. (2011). Comparison of Methods for Land-Use Classification Incorporating Remote Sensing and GIS Inputs. Applied Geography, 31(2), 533–544. https://doi.org/10.1016/j.apgeog.2010.11.006

Sadoddin, A., Sheikh, V., Mostafazadeh, R., & Halili, M. (2010). Analysis of vegetation-based management scenarios using MCDM in the Ramian watershed, Golestan, Iran. International Journal of Plant Production, 4(1), 51–62. https://doi.org/10.22069/ijpp.2012.681

Sakieh, Y., & Salmanmahiny, A. (2016). Performance assessment of geospatial simulation models of land-use change—a landscape metric-based approach. Environmental Monitoring and Assessment, 188(3), 169. https://doi.org/10.1007/s10661-016-5179-5

Turner, M. G. (1989). Landscape ecology: The effect of pattern on process. Annual Review of Ecology and Systematics, 20, 171–197. https://doi.org/10.1146/annurev.es.20.110189.001131

Uddin, K., Abdul Matin, M., & Maharjan, S. (2018). Assessment of land cover change and its impact on changes in soil erosion risk in Nepal. Sustainability, 10(12), 4715. https://doi.org/10.3390/su10124715

Uuemaa, E., Antrop, M., Roosaare, J., Marja, R., & Mander, U. (2009). Landscape metrics and indices: An overview of their use in land scape research. Living Reviews in Landscape Research, 3(1), 1–18. https://text2fa.ir/wp-content/uploads/Text2fa.ir-Landscape-Metrics-and-Indices-1.pdf

Van Vliet, J., Bregt, A. K., & Hagen-Zanker, A. (2011). Revisiting Kappa to account for change in the accuracy assessment of land-use change models. Ecological Modelling, 222(8), 1367–1375. https://doi.org/10.1016/j.ecolmodel.2011.01.017

Vlachogianni, S., Servou, A., Karalidis, K., Paraskevis, N., Menegaki, M., & Roumpos, C. (2025). Remote sensing-based monitoring of land use and cover dynamics in surface lignite mining regions: A supervised classification approach. Earth Science Informatics, 18, 256. https://doi.org/10.1007/s12145-025-01781-5

Walz, U. (2011). Landscape structure, landscape metrics and biodiversity. Living Reviews in Landscape Research 5(3), 1–35. http://dx.doi.org/10.12942/lrlr-2011-3

Wei, X., Xiao, Z., Li, Q., Li, P., & Xiang, C. (2016). Evaluating the effectiveness of landscape configuration metrics from landscape composition metrics. Landscape and Ecological Engineering, 13(1), 169–181. https://doi.org/10.1007/s11355-016-0314-6

Yang, D., Zhang, P., Zhang, J., Liu, Y., Liu, Z., & Chen, Z. (2025). Land use assessment under dynamic evolution: Multi-objective optimization and multi-scenario simulation analysis. Journal of Environmental Management, 373, 123456. https://doi.org/10.1016/j.jenvman.2024.123456

Zabihi, M., Moradi, H. R., Gholamalifard, M., & Khaledi Darvishan, A. (2019). Effects of Land Use/Land Cover Change Scenarios on Landscape Metrics on the Talar Watershed. Watershed Management Research Journal, 32(1), 84–99. https://doi.org/10.22092/wmej.2018.123624.1156

Zabihi, M., Moradi, H. R., Gholamalifard, M., Khaledi Darvishan, A., & Fürst, C. (2020). Landscape Management through Change Processes Monitoring in Iran, Sustainability 12(5), 1753. https://doi.org/10.3390/su12051753

Zabihi, M., Mostafazadeh, R., & Sedaghati Gonabadi, I. (2025). Analyzing the spatial patterns and changes in urban green spaces of an under rapid urbanization area through landscape metrics. Advances in Space Research, 76(5), 2779–2794. https://doi.org/10.1016/j.asr.2025.06.063

Zhang, H., Yan, Q., Xie, F., & Ma, S. (2023). Evaluation and prediction of landscape ecological security based on a CA-Markov model in overlapped area of crop and coal production. Land, 12(1), 207. https://doi.org/10.3390/land12010207

Article first received: 12 June 2025
Article accepted: 13 February 2026